Concentration dependence of shape and structure fluctuations of droplet microemulsions investigated by neutron spin echo spectroscopy

Michihiro Nagao[1,2,*] and Hideki Seto[3,†]

[1]*NIST Center for Neutron Research, National Institute of Standards and Technology, Gaithersburg, Maryland 20899-6102, USA*

[2]*Cyclotron Facility, Indiana University, Bloomington, Indiana 47408-1398, USA*

[3]*Department of Physics, Graduate School of Science, Kyoto University, Kyoto, 606-8502, Japan*

(Received 2 January 2008; published 28 July 2008)

We describe dynamic modes that originate from shape and structure fluctuations in a droplet microemulsion system. The modes are decoupled by a contrast variation neutron scattering technique using the relative intermediate form factor method. The strategy of the method is analogous to the relative form factor method, which decouples the form and structure factors from the small-angle neutron scattering intensity [M. Nagao *et al.*, Phys. Rev. E **75**, 061401 (2007)]. First, we will briefly explain theoretical and experimental approaches to understanding neutron spin echo (NSE) data from droplet microemulsion systems. Then we will introduce the relative intermediate form factor method, which decouples shape and structure fluctuations. The concentration dependence of the droplet dynamics in a microemulsion system is used to elucidate the strengths of this method. The intermediate form and structure factors are successfully decoupled from an observed intermediate scattering function by NSE. The decay rate of the shape fluctuation modes linearly decreases, while the fluctuation amplitude increases as the droplet concentration increases. The first cumulant of the obtained intermediate structure factor shows a clear de Gennes narrowing behavior at a length scale corresponding to the interdroplet distance. However, in the high-momentum-transfer and longer-time regions, the first cumulant deviates from the intermediate structure factor. This result suggests the existence of other dynamic modes of structure fluctuations rather than the center-of-mass diffusion mode.

DOI: 10.1103/PhysRevE.78.011507 PACS number(s): 61.05.fg, 82.70.Uv, 87.16.dj

I. INTRODUCTION

The dynamic behavior of amphiphilic membranes has been investigated by many researchers to understand self-assembling mechanisms of the systems. Not only static structures, but also dynamic behaviors are quite important to understand the physical properties of such systems, since those membranes thermally fluctuate and the fluctuations are essential for self-assembly. Lipid membranes are typical examples of bilayer systems, where the rigidity is an issue in understanding the properties of complex biological membranes. Since biological systems are constructed in crowded environments, understanding the thermal fluctuations of membranes under crowded environments is one of the important challenges in soft-matter physics.

The most successful model to describe membrane fluctuations was proposed by Milner and Safran in 1987 [1]. The dynamics of surfactant monolayer coated droplet microemulsions is described by a center-of-mass diffusion and shape fluctuations of the spherical droplets. The shape fluctuations of droplets are modeled within the treatment of Helfrich's bending Hamiltonian [2]. The Milner-Safran theory was applied to the result obtained by means of neutron spin echo (NSE) for the first time by Huang *et al.* [3], and the validity of their theory and the dynamic feature of microemulsion droplets have been clarified [3,4]. The estimated values of the bending modulus using the theory, however, were several times smaller than the expected values. In order to solve the problem, Hellweg and Langevin proposed a method to separate membrane fluctuations from the center-of-mass diffusion of droplets [5,6]. They used dynamic light scattering (DLS) to determine the center-of-mass diffusion constant, and a reasonable value of the bending modulus was estimated using NSE. They also pointed out the possibility of the combination with nuclear magnetic resonance (NMR) to estimate the self-diffusion constant [7]. Lisy and Brutovsky [8] and Farago and Gradzielski [9] claimed that the effect of shape fluctuations should be considered to explain the static form factor observed by small-angle scattering.

As has been demonstrated in the approaches mentioned above, mode decoupling between shape fluctuations and the center-of-mass diffusion is necessary for a quantitative evaluation of structure parameters. This helps us to understand self-assembling mechanisms in membrane systems within a nanosecond time window even in dilute droplet systems. When the concentration of droplets increases, the center-of-mass diffusion should be reduced due to interdroplet potentials and hydrodynamic interactions, and therefore, reduce the structure factor fluctuations. This fact implies that the center-of-mass diffusion constant is no longer momentum transfer, q, independent, but a q-dependent quantity. Although several experimental works in crowded colloidal systems have been made by some groups [10–14], no q dependence of the diffusion constant has been described, except for the results by Gazeau *et al.* [15] and Häußler and Farago [16].

In order to decouple shape and structure fluctuations, the contrast variation neutron scattering technique is suitable.

*mnagao@indiana.edu

†Present address: Institute of Materials Structure Science, High Energy Accelerator Research Organization, Tsukuba 305-0801, Japan.

Molle and co-workers [13,14] used contrast-variation NSE to understand the dynamics of droplets in a cubic microemulsion. They measured NSE data for several scattering contrast conditions including the matching point, where the scattering from the structure factor was matched out. This data allowed them to discuss shape fluctuation modes of their system. They concluded that the frequency of shape fluctuations increases in crowded environments.

Another way to derive such information is to extend the relative form factor method for contrast-variation small-angle neutron scattering (SANS) data analyses [17–20] into dynamic mode decoupling. Using the contrast-variation SANS technique, a ratio of scattering intensities for two different contrast conditions is defined as the relative form factor, which is the ratio of the form factors for each contrast condition. Therefore, without any assumption about the structure factor, the form factor can be evaluated. Once the form factor is known, the structure factor can be calculated from the scattering intensity. In this procedure it is not necessary to measure at the matching point, but simply at two scattering contrast conditions that give clear changes in the apparent shape of the form factors.

In this paper, therefore, we discuss a contrast-variation NSE result obtained in a water-in-oil droplet microemulsion consisting of dioctyl sulfosuccinate sodium salt (AOT), water, and decane. While keeping the radius of water droplets constant, the water droplet concentration ϕ was changed from 5% to 60%. Introducing a relative intermediate form factor, which is the ratio of intermediate scattering functions between different scattering contrasts, modes from shape fluctuations are decoupled with those from structure fluctuations. The decay rate and the fluctuation amplitude of the membrane dynamics tend to decrease and increase, respectively, with increasing ϕ. The bending modulus of membranes, κ, is extracted within the theoretical framework for single-droplet dynamics [1]. Furthermore, the normalized intermediate structure factor $S(q,t)/S(q,0)$ is estimated in the crowded environment, where t is the time. The first cumulant of $S(q,t)/S(q,0)$ shows a clear dip of a diffusion constant around the q value corresponding to the interdroplet distance. The $S(q,t)/S(q,0)$ in the high-q and long-t regions shows a clear discrepancy from the first cumulant, and this suggests the existence of other dynamic modes of structure fluctuations.

II. THEORY

In dilute droplet microemulsion systems, Lovesey and Schofield proposed a single-particle shape fluctuation model [21]. This model was modified by Milner and Safran to apply the theory to NSE analyses [1]. They treated membrane fluctuations as spherical harmonics and derived the following intermediate scattering function [1]:

$$I(q,t) = \exp[-\Omega_0 t]V_s^2(\Delta\rho)^2\left[f_0(qR) + \sum_{l\geq 2}\frac{2l+1}{4\pi R^2}f_l(qR) \times\langle|u_l|^2\rangle\exp[-\Gamma_l t]\right], \quad (1)$$

where Ω_0 is the decay constant for the center-of-mass diffusion of droplets, V_s the volume of droplet, $\Delta\rho$ the scattering length density difference between droplet and solvent, R the mean radius of droplets, $\langle|u_l|^2\rangle$ the amplitude of fluctuations corresponding to the lth mode, and Γ_l the decay rate for the lth mode, respectively. The $f_0(qR)$ and $f_l(qR)$ are the static form factor of the zeroth and lth mode fluctuations, and the expressions for them are given later. In Eq. (1) the term $\exp[-\Omega_0 t]$ describes the center-of-mass diffusion of droplets [1,21] and the rest of the equation indicates the shape fluctuation modes of droplets. Thus, Eq. (1) can be rewritten as

$$I(q,t) = V_s^2(\Delta\rho)^2F(q,t)\exp[-\Omega_0 t], \quad (2)$$

where $F(q,t)$ is the intermediate form factor,

$$F(q,t) = f_0(qR) + \sum_{l\geq 2}\frac{2l+1}{4\pi R^2}f_l(qR)\langle|u_l|^2\rangle\exp[-\Gamma_l t]. \quad (3)$$

When droplet concentration increases, the simple diffusion mode changes to a mutual diffusion mode and $\Omega_0 = D_0 q^2$ changes to $\Omega = D(q)q^2$, where D_0 is the free-particle diffusion constant, $D_0 = k_B T/(6\pi\eta R_H)$, k_B, T, η, and R_H are the Boltzmann constant, temperature, solvent viscosity, and hydrodynamic radius of droplets, respectively, and $D(q)$ is the q-dependent diffusion constant. Thus, the term $\exp[-\Omega_0 t]$ is considered to originate from structure fluctuations—namely, the intermediate structure factor $S(q,t) \propto \exp[-\Omega_0 t]$. Therefore, the normalized intermediate scattering function $I(q,t)/I(q,0)$ is a product of the normalized intermediate form and structure factors $F(q,t)/F(q,0)$ and $S(q,t)/S(q,0)$ as

$$\frac{I(q,t)}{I(q,0)} = \frac{F(q,t)}{F(q,0)}\frac{S(q,t)}{S(q,0)}. \quad (4)$$

To simplify our discussion, we assume that shape and structure fluctuations are independent. However, this is not strictly true in crowded microemulsion systems, since interdroplet interactions affect the shape fluctuations of droplets. In crowded environments, the theory describing droplet dynamics has to be modified. The coupling of each dynamic mode makes Eq. (4) more complicated and the simple expression is not valid. Although we do not know the limitation of the validity of Eq. (4) so far, this form may be valid in some cases. The simplest case is the spherical droplet microemulsion, since the system has rotational symmetry and all modes are identical between different particles. The purpose of the present paper is to show the idea of data treatment, and thus, the simplest arguments are chosen to evaluate the dynamics of droplets.

Expression (4) is quite similar to the expression for SANS profiles from spherical droplet microemulsions—namely, $I(q) = nF(q)S(q)$, where n is the number density of scatterers. In the case of droplet microemulsion systems, the validity of the relative form factor method has been confirmed in small polydispersity cases [17–20]. Contributions from the form factor and structure factor can be decoupled from SANS intensities by this method. Here, the same strategy is applied to intermediate scattering functions.

When we measure NSE signals for different scattering contrast conditions with the same composition of samples,

the terms Ω_0 and Ω, which are the contributions from $S(q,t)/S(q,0)$, can be treated as identical. The difference of Ω_0 or Ω between different scattering contrasts arises from the difference of values of D_0, which originates from the viscosity difference due to the change of the dispersed medium. In the present case, the difference of the viscosities is relatively small (about 8%) and we can safely neglect it. Then the relative intermediate form factor $R(q,t)$ is defined as

$$R(q,t) \equiv \frac{[I(q,t)/I(q,0)]_b}{[I(q,t)/I(q,0)]_f} \approx \frac{[F(q,t)/F(q,0)]_b}{[F(q,t)/F(q,0)]_f}, \tag{5}$$

where the subscripts b and f indicate bulk contrast, which is a mixture of D_2O with hydrogenated oil and surfactant, and film contrast, which is a mixture of deuterated water and oil with hydrogenated surfactant, respectively. In bulk contrast cases, only water cores are visible by neutrons when a water-in-oil droplet microemulsion is formed. On the other hand, only surfactant membranes are visible by neutrons in film contrast cases, and it has been believed that the shape fluctuations of surfactant membranes is better proved in the film contrast samples [9].

Neglecting the shape fluctuation mode corresponding to $l>2$, the decaying function of shape fluctuation is expressed as

$$\frac{F(q,t)}{F(q,0)} = \frac{4\pi f_0(qR) + 5f_2(qR)\langle|a_2|^2\rangle \exp[-\Gamma_2 t]}{4\pi f_0(qR) + 5f_2(qR)\langle|a_2|^2\rangle}, \tag{6}$$

where

$$\langle|a_2|^2\rangle = \langle|u_2|^2\rangle/R^2. \tag{7}$$

The following equations apply for the static form factors:

$$f_0^b(qR) = \left[\frac{3j_1(qR)}{qR}\right]^2, \tag{8}$$

$$f_2^b(qR) = [3j_2(qR)]^2, \tag{9}$$

$$f_0^f\{q(R+\delta)\} = [j_0\{q(R+\delta)\}]^2, \tag{10}$$

$$f_2^f\{q(R+\delta)\} = [4j_2\{q(R+\delta)\} - \{q(R+\delta)\}j_3\{q(R+\delta)\}]^2, \tag{11}$$

where δ is the surfactant layer thickness and $j_n(x)$ is the spherical Bessel function of order n.

In the present method, the best way to fit the NSE data is to perform the fit of $R(q,t)$ according to Eq. (5) with Eq. (6) taking the effect of polydispersity into account. In this paper, however, the simplest data treatment is used, which is an approximated analysis method within the frame work of Milner-Safran theory [1]. The equation for the normalized intermediate scattering function is as follows:

$$\frac{I(q,t)}{I(q,0)} \approx \exp[-\Gamma_{\text{eff}}(q)t] = \exp[-D_{\text{eff}}(q)q^2 t]. \tag{12}$$

Equation (12) is equivalent to the first cumulant of Eq. (1), where $\Gamma_{\text{eff}}(q)$ and $D_{\text{eff}}(q)$ are the effective decay rate and the effective diffusion constant, respectively. $D_{\text{eff}}(q)$ contains two contributions from $D(q)$ and deformational diffusion constant $D_{\text{def}}(q)$ as $D_{\text{eff}}(q)=D(q)+D_{\text{def}}(q)$. $D_{\text{def}}(q)$ is expressed as

$$D_{\text{def}}(q) = \frac{5f_2(qR)\langle|a_2|^2\rangle\Gamma_2}{4\pi f_0(qR) + 5f_2(qR)\langle|a_2|^2\rangle}. \tag{13}$$

Finally, we obtain $R(q,t)$ as follows:

$$R(q,t) \equiv \frac{[I(q,t)/I(q,0)]_b}{[I(q,t)/I(q,0)]_f} \tag{14}$$

$$\approx \exp[-\Gamma_{\text{rel}}(q)t] = \exp[-D_{\text{rel}}(q)q^2 t], \tag{15}$$

where

$$\Gamma_{\text{rel}}(q) = \Gamma_{\text{eff}}^b(q) - \Gamma_{\text{eff}}^f(q), \tag{16}$$

$$D_{\text{rel}}(q) = D_{\text{eff}}^b(q) - D_{\text{eff}}^f(q) = D_{\text{def}}^b(q) - D_{\text{def}}^f(q). \tag{17}$$

Note that we assume that the $D(q)$'s of both scattering contrasts are identical.

Using the above procedure, the dynamic parameters for shape fluctuation modes are evaluated. The intermediate form factor can be calculated by putting the parameters into Eq. (6). Dividing $I(q,t)/I(q,0)$ by $F(q,t)/F(q,0)$ one can decouple $S(q,t)/S(q,0)$. Once the intermediate structure factor is obtained, we can analyze structure fluctuation modes which include information about interactions between droplets.

In cases of interacting Brownian particles, Pusey [22] and Ackerson [23,24] discussed the intermediate scattering function observed by DLS. They considered a situation that the time scale is long compared to the time between solvent molecule and Brownian particle collisions, but short compared to the time between the collisions of Brownian particles with each other [24], and proposed the following relation:

$$\frac{S(q,t)}{S(q,0)} = \exp[-D_0 q^2 t/S(q,0)]. \tag{18}$$

The above equation explained some experimental results [25]. Since this time scale corresponds to the NSE time scale as well, we employ this relation to describe the structure fluctuation mode in the present paper. Taking the first cumulant of $S(q,t)/S(q,0)$, the following relation with $D(q)$ is obtained [26]:

$$D(q) = -\frac{1}{S(q,0)q^2}\left[\frac{\partial S(q,t)}{\partial t}\right]_{t=0}, \tag{19}$$

where the q dependence of the diffusion constant, $D(q)$, is $D(q)=D_0/S(q)$ under the assumption of Eq. (18). In some cases a modification to include hydrodynamic effects is necessary [23,26–29], and the apparent $D(q)$ has the following relation [28]:

$$D(q) = D_0 \frac{H(q)}{S(q)}, \tag{20}$$

where $S(q)$ and $H(q)$ are the structure factor and hydrodynamic effect, respectively. Although $H(q)$ has been evaluated in some colloidal systems so far [15,16], hydrodynamic effects in microemulsion systems still remain as an unsolved issue of soft-matter systems.

It is noted that the treatment below Eq. (12) is similar to the ratio of decay rates of the first cumulant done by Holderer *et al.* for a bicontinuous microemulsion [30]. They indicated that the ratio of their decay rates obtained from bulk and film contrast samples showed a dip at a finite q. Although they mentioned that their dip originated from the different dynamic behaviors between different scattering contrasts, they did not discuss its physical meaning. In this paper, therefore, we show the physical meaning of the ratio of different scattering contrast data for droplet microemulsion systems.

III. EXPERIMENT

The concentration dependence of the dynamic behavior of a droplet microemulsion system was investigated in an AOT microemulsion. AOT (purity 99%) was purchased from Fluka, D_2O (atomic fraction of deuterium of 99.9%), deuterated *n*-decane (atomic fraction of deuterium of 99%) from Isotec Inc., and *n*-decane (purity 99%) from Katayama Chemical Co.[1] These materials were mixed by weight without any further purification. The molar ratio of D_2O and AOT was kept at 38.2, and the droplet concentration ϕ was 0.05, 0.3, and 0.6. The static structure of these concentration samples has been investigated in our previous SANS experiment [18,19]. Two different scattering contrast samples were prepared; one was the bulk contrast ($AOT/D_2O/C_{10}H_{22}$ for ϕ=0.3 and 0.6 or $AOT/H_2O/C_{10}D_{22}$ for ϕ=0.05) and the other was the film contrast ($AOT/D_2O/C_{10}D_{22}$). The characteristic feature of the system has been well investigated by many researchers [10,12,31–38].

The NSE experiment was done using the ISSP-NSE spectrometer in Tokai, Japan [39,40], and NG5-NSE spectrometer at the NIST Center for Neutron Research [41,42]. The measured spatial and time domains for ISSP-NSE were from 0.02 to 0.1 Å^{-1} and from 0.1 ns to 15 ns, and those for NG5-NSE were from 0.03 to 0.12 Å^{-1} and from 0.05 ns to 40 ns, respectively. The temperature was kept constant at room temperature, $T=(25.0\pm0.3)$ °C. The DAVE software package was used for elements of the data reduction and analysis for the NG5-NSE data [43].

IV. RESULTS AND DISCUSSION

A. Classical data treatment

Figure 1 shows the observed $I(q,t)/I(q,0)$ from the AOT microemulsion with ϕ=0.3 for (a) the bulk contrast and (b) the film contrast, respectively. Comparing each graph, the following arguments are realized. The decay in the film contrast sample is slower than that in the bulk contrast in the high-q region. At $q\approx0.05$ Å^{-1}, the decay in the film contrast sample is faster than that in the bulk contrast. This q value corresponds to $qR\approx\pi$, and therefore, the shape fluctuations of droplets are enhanced at this q [3,9]. The solid lines in the figure are fits according to Eq. (12).

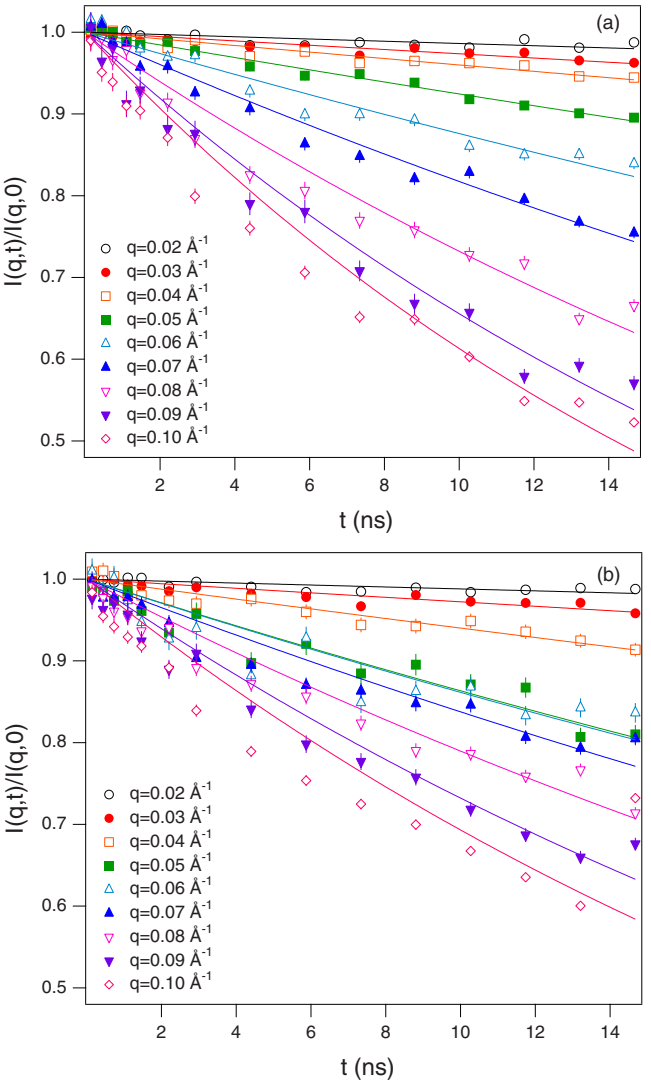

FIG. 1. (Color online) Observed $I(q,t)/I(q,0)$ from (a) the bulk contrast and (b) the film contrast samples in AOT microemulsion with a droplet concentration ϕ of 0.3. The solid lines indicate the fit results according to a single-exponential function. The error bars shown in this text indicate ±1 standard deviation.

Figure 2 shows the evaluated $D_{\rm eff}(q)$ and SANS profile for ϕ=0.3 obtained for (a) the bulk and (b) film contrast samples [18,19]. $D^b_{\rm eff}(q)$ in Fig. 2(a) shows a dip at $q\approx0.04$ Å^{-1}, and the corresponding SANS profile shows a slight shoulder. Therefore, the dip in $D^b_{\rm eff}(q)$ expresses so-called "de Gennes narrowing" due to the effect of the scattering peak [44]. This dip in $D^b_{\rm eff}(q)$ arises from the structure fluctuation modes. On the other hand, a peak in $D^f_{\rm eff}(q)$ is observed in the film contrast sample, and the corresponding SANS profile shows a dip at $q\approx0.05$ Å^{-1}, as shown in Fig.

[1]Certain commercial equipment, instruments, or materials are identified in this paper to foster understanding. Such identification does not imply recommendation or endorsement by the National Institute of Standards and Technology, nor does it imply that the materials or equipment identified are necessarily the best available for the purpose.

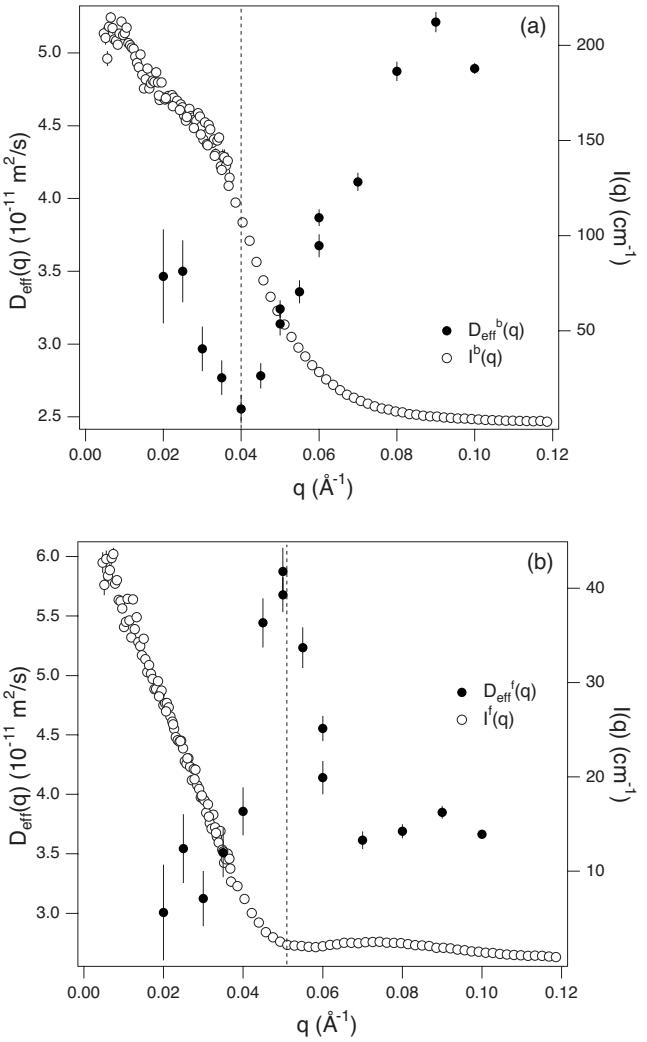

FIG. 2. $D_{\mathrm{eff}}(q)$ and SANS profile from $\phi=0.3$ for (a) the bulk contrast and (b) the film contrast. SANS data shown here are the same data as the previous publication [19]. Dashed vertical lines are shown to guide the eye.

2(b). This peak in $D_{\mathrm{eff}}^f(q)$ originates from the dynamic mode corresponding to the shape fluctuations of droplets.

So far, in order to analyze these data some assumptions are necessary; for example, the mode of shape fluctuation is the same as that of the dilute droplet systems, or D_0 is calculated from the Stokes-Einstein relation, etc., since both the contributions from shape and structure fluctuation modes are observed as a coupling of each other. These assumptions are essential in understanding the dynamic nature of systems. Especially, interactions between droplets should affect the q dependence of the diffusion constant, while the effect of such interactions on the dynamic behavior of microemulsion systems has not been clarified yet.

In the present case, it is obvious that both the shape and structure fluctuations show q dependences, and these modes affect the NSE data in both scattering contrasts. The q dependence of the center-of-mass diffusion constant cannot be evaluated by any other experimental techniques in our q range, although DLS or NMR will give us the value of the q-independent self-diffusion constant [5–7]. If we directly

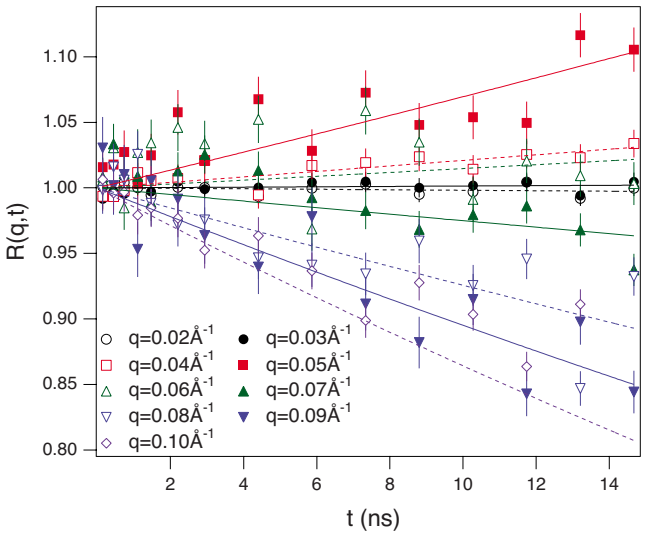

FIG. 3. (Color online) Evaluated $R(q,t)$ for AOT microemulsion of $\phi=0.3$. The lines are the fit result according to Eq. (15).

estimate parameters for the shape fluctuation modes from the data shown in Fig. 2(b), we will underestimate them due to the structure fluctuation modes. Also the structure fluctuation modes will be underestimated due to the shape fluctuation modes if we try to estimate parameters from the result shown in Fig. 2(a). This means that the shape and structure fluctuation modes are obtained as a coupling of each component in the scattering experiment and are not possible to discuss separately in the classical data treatment. We will now describe the results of the data analysis using $R(q,t)$, which method allows one to discuss the fluctuation modes independently from each other.

B. Decoupling shape and structure fluctuations

Dividing two intermediate scattering functions with different scattering contrast following Eq. (5), we obtain $R(q,t)$ for $\phi=0.3$, as shown in Fig. 3. The lines indicate the fit results according to the single-exponential function, Eq. (15). Since $R(q,t)$ indicates the ratio of $I(q,t)/I(q,0)$'s between the bulk and film contrast samples, $R(q,t)=1$ means that both of them are the same. When $R(q,t)$ is larger than 1 [$\Gamma_{\mathrm{rel}}(q)$ is negative], the contribution from the film contrast sample is larger than that from the bulk contrast or vice versa. In this way, different dynamic behaviors between different scattering contrast samples are emphasized.

Figure 4 shows the q dependence of $\Gamma_{\mathrm{rel}}(q)$ obtained from the fit of $R(q,t)$. The relative form factor [19] $R(q)$ for $\phi=0.3$ is also shown in the figure. Interestingly, the shape of $\Gamma_{\mathrm{rel}}(q)$ seems the inverse of the shape of $R(q)$. This means that the relative intermediate form factor method has a clear correlation with the relative form factor method. Here the fit parameters are $\langle|a_2|^2\rangle$ and Γ_2. Within the theory of membrane fluctuation dynamics [45,46] these parameters are expressed as follows:

$$\langle|a_2|^2\rangle = \frac{k_BT}{4\kappa}\left[4\frac{R}{R_s} - 3\frac{\bar{\kappa}}{\kappa} - \frac{3k_BT}{4\pi\kappa}f(\phi)\right]^{-1}, \qquad (21)$$

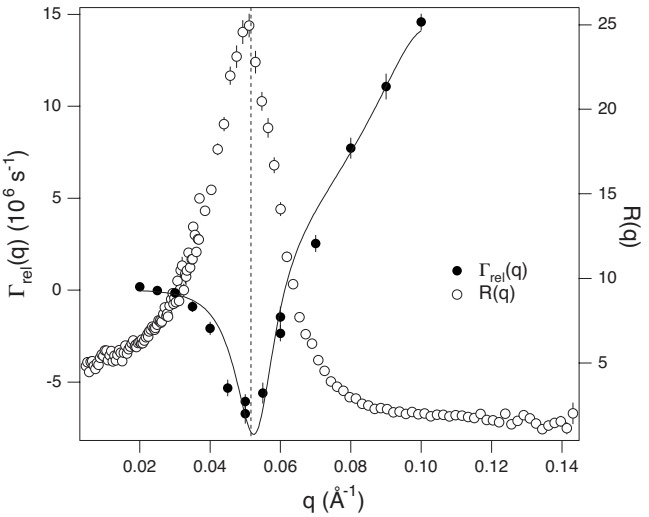

FIG. 4. Obtained $\Gamma_{rel}(q)$ and $R(q)$. The q values of the peak of $R(q)$ and the dip of $\Gamma_{rel}(q)$ are at almost the same q. The $R(q)$ data are the same as used in the previous work [19]. The solid line indicates the fit result of $\Gamma_{rel}(q)$ according to Eq. (16).

$$\Gamma_2 R^3 = \left[4\frac{R}{R_s} - 3\frac{\bar{\kappa}}{\kappa} - \frac{3k_BT}{4\pi\kappa} f(\phi) \right] \frac{24\kappa}{23\eta_c + 32\eta_s}, \quad (22)$$

where R_s^{-1}, $\bar{\kappa}$, and $f(\phi)$ are the spontaneous curvature of membranes, the saddle-splay modulus, and the entropic contribution to the free energy due to ϕ. It should be noted here that the effects from $\bar{\kappa}$ and $f(\phi)$ are included in the free-energy functional in the present data treatment. $\eta_c = 1.10 \times 10^{-3}$ Pa s and $\eta_s = 0.87 \times 10^{-3}$ Pa s for bulk contrast and 0.94×10^{-3} Pa s for film contrast are the viscosities inside (droplet core) and outside (solvent) of droplets. All the terms on the right-hand side of Eqs. (21) and (22) are contrast independent. Although the parameters R, η_c, and η_s depend on scattering contrast, the small difference of viscosities can be neglected and normally $R \ll R_s$ is satisfied. In this case the difference of R/R_s is negligible between different scattering contrasts. Therefore, we used the assumption $\Gamma_2^f (R+\delta)^3 \approx \Gamma_2^b R^3$, where Eq. (22) is assumed to be contrast independent. To fit $\Gamma_{rel}(q)$, we put $R = (43.6 \pm 0.6)$ Å and $R+\delta = (59.7 \pm 0.5)$ Å from the previous SANS result [19]. The best-fit values for those parameters for $\phi = 0.3$ are $\langle |a_2|^2 \rangle = (7.8 \pm 0.7) \times 10^{-2}$ and $\Gamma_2^b = (2.29 \pm 0.06) \times 10^7$ s^{-1}.

Using these parameters and Eq. (13), the deformational diffusion constant $D_{def}(q)$ is extracted. Figure 5 shows $D_{def}(q)$ and the calculated $F(q)$ using the structure parameters obtained before [19] for both the contrasts. $D_{def}(q)$ of the film contrast shows a clear peak at $q \approx 0.05$ Å^{-1}. This q value is the same as that of the dip position in $F(q)$. On the other hand, $D_{def}(q)$ of the bulk contrast grows as q increases, probably resulting from the enhanced shape fluctuations. The first dip of the form factor in the bulk contrast is calculated to be around 0.12 Å^{-1} (not shown). At the dip position the enhancement of the shape fluctuation mode should be observed. However, the scattering intensity from bulk contrast samples is often low at high q and thus makes it difficult to analyze the data. Therefore shape fluctuation modes have

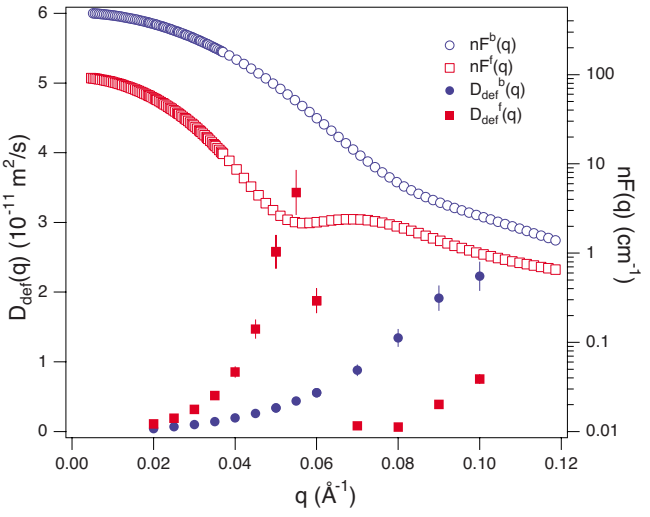

FIG. 5. (Color online) Comparisons between the static form factor calculated in Ref. [19] and $D_{def}(q)$ for $\phi = 0.3$ of both contrasts. The deformation motion is enhanced at the same q value as the dip position of the SANS profile. This tendency is much more visible in the film contrast data.

been estimated using the film contrast conditions.

Using Eq. (6) and the estimated dynamic parameters, $F(q,t)/F(q,0)$ can be calculated as shown in Fig. 6 for $\phi = 0.3$ with bulk and film contrasts. The error bars are not shown in the figure for better visualization, and they are dominated by the error of $\langle |a_2|^2 \rangle$, which is about 10%. In the case of the bulk contrast, the decaying function follows the order of the q values since the diffusion constant is a monotonic increasing function with q as shown in Fig. 5. On the other hand, in the case of the film contrast, $D_{def}^f(q) \approx 0$ at $q = 0.08$ Å^{-1} (see Fig. 5), and thus the decay in $F(q,t)/F(q,0)$ is slower than that at lower q (Fig. 6). Dividing $I(q,t)/I(q,0)$

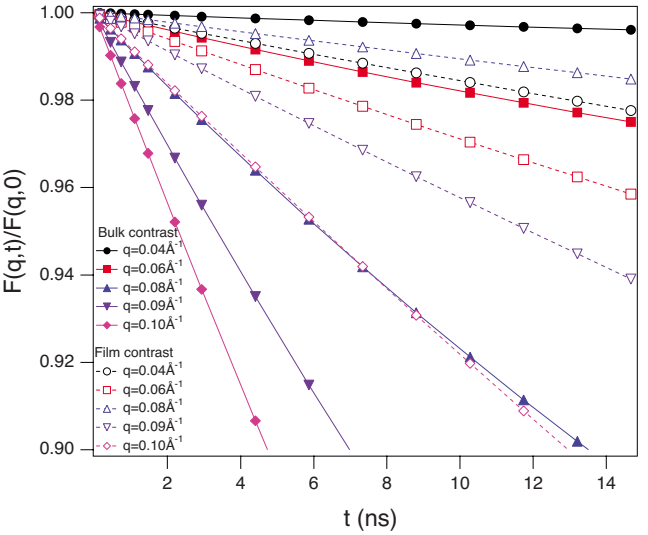

FIG. 6. (Color online) Obtained $F(q,t)/F(q,0)$ for $\phi = 0.3$. Solid symbols are those of bulk contrast and open symbols are of film contrast, respectively. The error bars are not shown in this figure for better visualization. The error bars are dominated by the error of $\langle |a_2|^2 \rangle$ of about 10%.

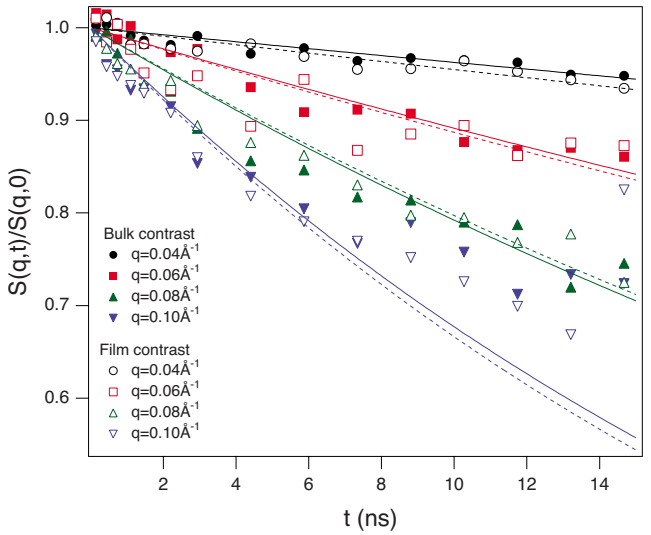

FIG. 7. (Color online) Obtained $S(q,t)/S(q,0)$ for $\phi=0.3$. Solid symbols are those of bulk contrast and open symbols are of film contrast, respectively. The error bars are not shown in this figure for better visualization. The error bars are dominated by the error of $\langle|a_2|^2\rangle$ of about 10%. The solid and dashed lines are fit results according to Eq. (23).

of Fig. 1 by $F(q,t)/F(q,0)$ of Fig. 6, $S(q,t)/S(q,0)$ is decoupled from $I(q,t)/I(q,0)$ as shown in Fig. 7. The figure shows the q variation of $S(q,t)/S(q,0)$ of $\phi=0.3$ for both contrast conditions. Almost identical decay functions are obtained for the different scattering contrasts at the same q. This is evidence of the validity of the present data reduction method.

The solid (bulk contrast) and dashed (film contrast) lines in Fig. 7 indicate fit results according to the first cumulant analyses using the following relation:

$$\ln[S(q,t)/S(q,0)] = -D(q)q^2t. \tag{23}$$

The diffusion constant $D(q)$ is estimated from the fit and shown in Fig. 8. The solid symbols in Fig. 8 indicate $D(q)$ for $\phi=0.3$ of the bulk contrast case. A clear dip is observed at $q\approx0.04$ Å^{-1}. This position is almost identical to the dip position of $D^b_{\rm eff}(q)$ in Fig. 2(a) as well as the peak position in $S(q)$. This result indicates that a clear de Gennes narrowing is evaluated from a simple analysis of $S(q,t)/S(q,0)$.

The open symbols in Fig. 8 show the q dependence of the diffusion constant, $D'(q)=D_{\rm eff}(q)-D_{\rm def}(q)$, of $\phi=0.3$ for the bulk contrast. Here $D_{\rm eff}(q)$ was evaluated by a fit of $I(q,t)/I(q,0)$ shown in Fig. 1. Both $D(q)$ and $D'(q)$ are almost identical except at high q. As shown in Fig. 7, $S(q,t)/S(q,0)$ is explained using the single-exponential function. However, this function fails to explain the data in the high-q region. Figure 9 shows a typical example of the first cumulant analysis for $\phi=0.3$ at $q=0.10$ Å^{-1} of the bulk contrast sample. A clear deviation from the first cumulant is obtained in the longer-time region. This suggests the existence of other structure fluctuation modes rather than the center-of-mass diffusion mode. In order to discuss these structure factor fluctuations, the combinations with DLS and/or NMR are probably useful to determine the concentration dependence of the self-diffusion constant [5–7] as well as the existence of the other modes. This point should be carefully discussed in the future to understand the self-assembly of microemulsions in crowded environments.

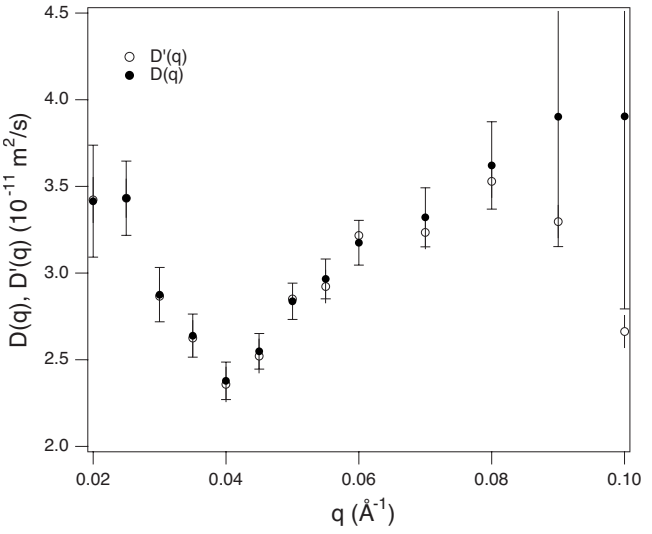

FIG. 8. Obtained q dependence of $D(q)$ and $D'(q)$ for $\phi=0.3$.

C. Concentration dependence of the dynamics

As we have shown above, the relative intermediate form factor method works well for the AOT droplet microemulsion system in the semidilute droplet range. We analyzed all concentration data at $\phi=0.05$, 0.3, and 0.6 using the same procedure and obtained parameters for the shape and structure fluctuations. In this section we focus our discussion on the concentration dependence of such parameters.

Figure 10 shows the ϕ dependence of best-fit parameters for the shape fluctuation mode. $\langle|a_2|^2\rangle$ increased while Γ^b_2 decreased with ϕ. These values are comparable to the results

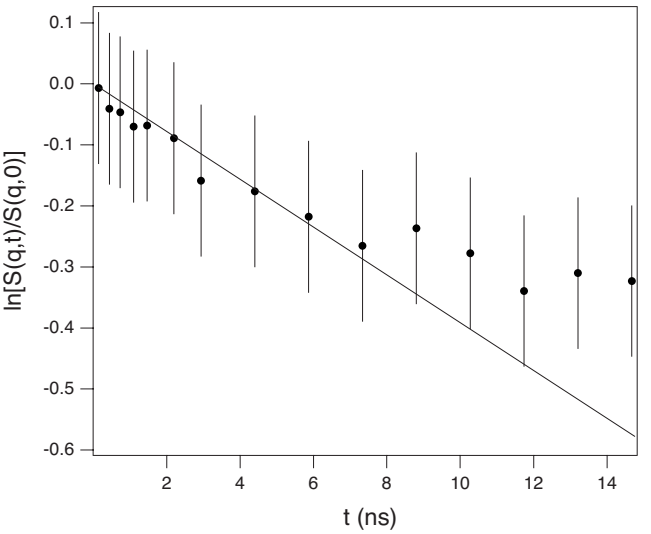

FIG. 9. Typical example for the first cumulant analysis for the bulk contrast sample of $\phi=0.3$ at $q=0.10$ Å^{-1}. The solid straight line indicates the linear fitting to the first cumulant. In the longer-time region, a clear deviation from the line is obvious.

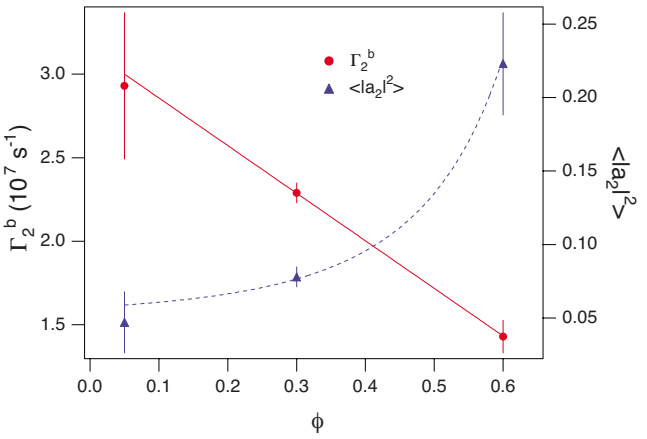

FIG. 10. (Color online) Concentration dependence of best-fit parameters for the shape fluctuation mode, Γ_2^b and $\langle|a_2|^2\rangle$. The solid and dashed lines are the fit results according to Eq. (24) or (25).

of Kawabata *et al.* [45]. They showed a set of Γ_2^b and $\langle|a_2|^2\rangle$ values of 2.0×10^8 s^{-1} and 0.1 in an AOT microemulsion with $R\approx33$ Å. Since Γ_2R^3=const is assumed, the values of Γ_2^b of the present case are expected to be around 0.5×10^8 s^{-1} for ϕ=0.05. The absolute value of Γ_2^b is smaller than our expectation. This problem might be due to the fit procedure of $R(q,t)$. $R(q,t)$ fully fitted by Eq. (5) with Eq. (6) considering the higher-order terms and the size polydispersity of droplets will improve the estimation of dynamic structure parameters.

Gang *et al.* [11] demonstrated a ϕ dependence of shape fluctuation modes in a sodium-dodecyl-sulfate/water/oil emulsion system using diffusing-wave spectroscopy. They employed a different model from the Milner-Safran theory [1], where the shape fluctuation mode is dominated by the interfacial tension. They explained the ϕ dependence of the relaxation rate and the amplitude of the shape fluctuation mode. In order to compare the present result with their result, we used a linear and a nonlinear relation of Γ_2^b and $\langle|a_2|^2\rangle$ against ϕ following their discussion [11].

For the ϕ dependence of the relaxation rate, Edwards and Schwartz predicted a linear form as a part of a theory for the nonlinear ϕ dependence of the effective viscosity of a deformable nondilute droplet suspension [47]. We employed an empirical linear ϕ dependence in Γ_2^b as [11]

$$\frac{\Gamma_2^b(\phi)}{\Gamma_2^b(0)} = 1 - a\phi. \tag{24}$$

The solid straight line in Fig. 10 is the best-fit result according to Eq. (24). The observed parameters are $\Gamma_2^b(0)=(3.1\pm0.1)\times10^7$ s^{-1} and $a=(0.91\pm0.08)$. The slope a is similar to the theoretical prediction of 1.4 [47] and the experimental observation by Gang *et al.* of 0.78 [11]. The result by Gang *et al.* [11] was obtained when the viscosities inside and outside the droplets differ by more than one order of magnitude, while the theory had approximately the same viscosities inside and outside the droplets. The conditions in the theory are close to the condition reported in this paper. The theory is best matched at $\phi\approx0.15$, and when the droplet concentration is too high, the theory is not appropriate [47]. The present result suggests that the direct contact of neighboring membranes affects the ϕ dependence of the parameter a, in addition to the velocity field of solvent, which is considered in the theory [47]. Our $\Gamma_2^b(0)$ is about an order of magnitude larger than that of Gang *et al.* [11]. This is because of the different bending elasticity of their emulsion and our microemulsion. The size of particles has a scaling relation with the bending elasticity—namely, larger scale objects have larger bending modulus. When membranes have larger bending modulus, the frequency of the shape fluctuation mode tends to be faster.

The present result shows only a slight increase of the frequency ($\tau=1/\Gamma_2^b$). On the other hand, Molle and coworkers [13,14] concluded that the shape fluctuation modes occur at one order of magnitude higher frequencies in crowded environments. Since they did not account for a concentration dependence in their work, more work is needed to justify these conclusions.

The increase of $\langle|a_2|^2\rangle$ with ϕ indicates the larger amplitudes of shape fluctuation modes in the higher-ϕ region. This result shows the same tendency as the result by Gang *et al.* [11]. Following their argument to discuss the ϕ dependence of the shape fluctuation amplitude, we employed the following equation [11]:

$$\frac{\langle|a_2(\phi)|^2\rangle}{\langle|a_2(0)|^2\rangle} = 1 + C\phi g(r;\phi), \tag{25}$$

where $g(r;\phi)$ is the pair correlation function evaluated at a constant distance of the droplet diameter. This relation is extracted from the following physical considerations. The shape fluctuations in the higher-ϕ region are enhanced due to the collision of neighboring droplets. This enhancement is energy driven, and the frequency of the collisions increases with increasing ϕ. The probability of two droplets colliding should scale with the number of pairs of droplets touching one another, which is given by $g(r;\phi)$ [11]. Following the treatment by Gang *et al.* [11], we used the form of $g(r;\phi)$ as the Carnahan-Starling equation of state for hard spheres [48,49]:

$$g(r;\phi) = \frac{1-\phi/2}{(1-\phi)^3}. \tag{26}$$

The dashed line in Fig. 10 shows the fit result according to Eq. (25). The best-fit parameters are $\langle|a_2(0)|^2\rangle=(0.057\pm0.008)$ and $C=(0.45\pm0.15)$. The present value of C is about 2 times larger than the value of Gang *et al.*, $C=0.2$ [11]. The value of amplitude of the shape fluctuations is one order of magnitude larger in the present result than the result by Gang *et al.* [11]. The difference in these parameters is due to the difference in the length scale and the solvent viscosity. They used oil-in-water emulsion whose oil core has about an order of magnitude larger viscosity than that of water. Their solvent, water, has a larger viscosity than our solvent, oil. In the case of smaller solvent viscosity, the collision of neighboring droplets occurs more easily than the case of higher solvent viscosity. This would make the parameter C larger in the present result. The ϕ dependence of

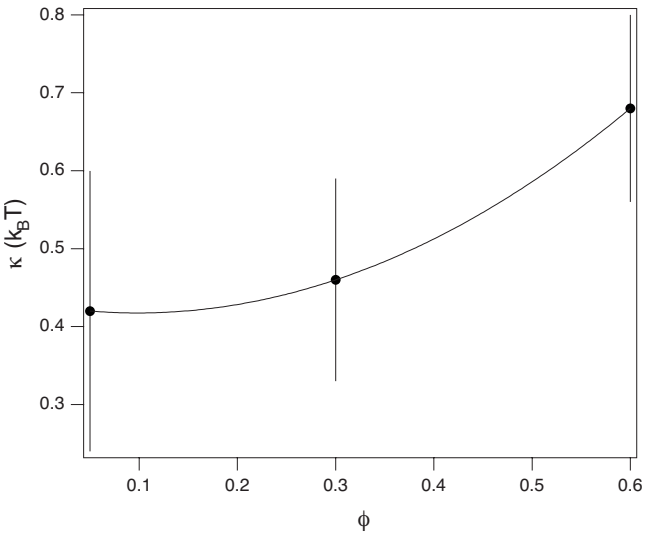

FIG. 11. Obtained ϕ dependence of the bending modulus κ. The solid line is a guide to the eye.

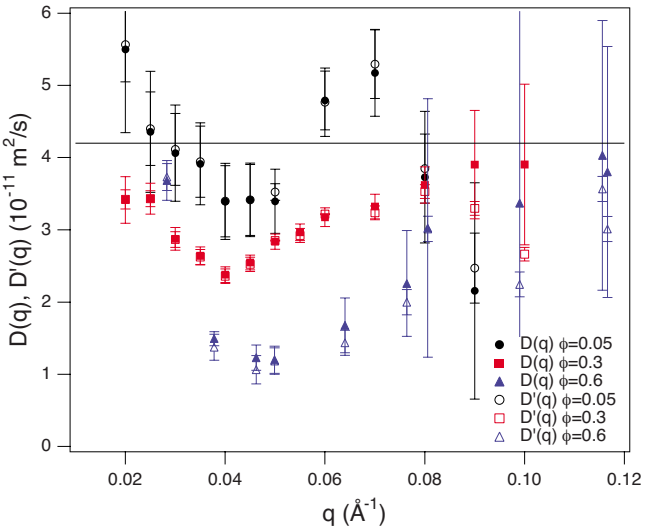

FIG. 12. (Color online) Obtained ϕ variation of $D(q)$ and $D'(q)$. The horizontal straight line is a theoretical value of D_0 from the Stokes-Einstein relation.

$\langle |a_2(\phi)|^2 \rangle$ is similar to the collision-driven shape fluctuations. However, as discussed by Gang *et al.*, several other physical origins may explain the present result [11].

It is worth discussing the concentration dependence of the bending modulus κ of the system from the observed parameters. We estimated κ following the single-droplet fluctuation model [1] as follows [45,50,51]:

$$\kappa = \frac{1}{48}\left(\frac{k_B T}{\pi p^2} + \Gamma_2 R^3 \frac{23\eta_c + 32\eta_s}{3}\right), \tag{27}$$

where p is the polydispersity index, and in the present concentrations, $p=(0.20\pm0.02)$, (0.16 ± 0.02), and (0.11 ± 0.01) were obtained for $\phi=0.05$, 0.3, and 0.6, respectively [19]. The resulting κ is shown in Fig. 11. The value of κ remains almost constant within the experimental error or may slightly increase with increasing ϕ. The bending rigidity of the surfactant membrane is not so much affected by the increase of ϕ. A slightly more rigid membrane in the high-ϕ region compared to that in the low ϕ region may be a reasonable conclusion. The absolute value of κ is smaller than the expected value ($\approx k_B T$) [52]. This is related to the errors in estimation of Γ_2^b as explained above.

Figure 12 shows the ϕ variation of $D(q)$ and $D'(q)$. The solid horizontal line indicates the value of $D_0=4.2\times10^{-11}$ m^2/s estimated from the Stokes-Einstein relation. Although the data points for $\phi=0.05$ are scattered, a slight dip in $D(q)$ is recognized, and its q value is almost the same as that where a small shoulder in $S(q)$ is obtained by SANS (see Fig. 5 of Ref. [19]). With increasing ϕ, the dip position shifts to higher q and it gets deeper. This is a reasonable result since the dip position is almost identical to the peak position in $S(q)$ (see Fig. 6 of Ref. [19]). This result indicates that the center-of-mass diffusion of droplets is suppressed at a length scale corresponding to the interdroplet distance. Another interesting feature here is that the dip positions of $D(q)$ for $\phi=0.05$ and 0.3 are almost identical. Previous SANS results showed that the peak position in $S(q)$ was almost constant below $\phi=0.4$. The present result supports the cluster-peak-like behavior in the low-ϕ region in AOT microemulsion systems as discussed in [19]. With the methodology proposed in this paper, one can start to study concentrated systems with interacting droplets which were shown to be important and complex in our earlier paper [19].

V. CONCLUSIONS

In this paper, we proposed a relative intermediate form factor method for contrast-variation neutron spin echo data analyses and discussed the concentration dependence of the dynamics in an AOT microemulsion system. Although some more modifications for quantitative discussion of membrane dynamics is necessary, shape and structure fluctuations are successfully decoupled in a droplet microemulsion system using this method. As a result, each fluctuation mode is discussed without an effect from the other fluctuation mode. The characteristic decay rate for the droplet shape deformation motion exhibits a linear decrease with ϕ, while the shape fluctuation amplitude shows a nonlinear increase. The ϕ dependence of the bending modulus κ is estimated and is almost constant or slightly increasing with ϕ. The bending rigidity of the surfactant membrane is not so much affected by an increase of the droplet concentration; a slightly more rigid surfactant membrane in the high-ϕ region may be a reasonable explanation for the ϕ dependence of κ. Using the estimated intermediate form factors, normalized intermediate structure factors $S(q,t)/S(q,0)$ in the dense droplet regime are evaluated. The first cumulant analysis is applied to the obtained $S(q,t)/S(q,0)$, and a clear dynamic slowing down is obtained at a length scale corresponding to the interdroplet distance. This behavior is consistent with the physical picture in crowded environments. In addition to this fact, the deviation of $S(q,t)/S(q,0)$ from the first cumulant suggests the existence of some other dynamic modes of structure fluctuations.

ACKNOWLEDGMENTS

The authors thank Dr. Jason S. Gardner and Dr. Steven R. Kline at NIST for their critical reading and the discussion of the manuscript. The NSE experiment at ISSP-NSE was done under approval of the Neutron Program Advisory Committee of Japan (Proposal No. 02.207). This work utilized facilities supported in part by the National Science Foundation under Agreement No. DMR-0454672. Financial support from U.S.-Japan Collaborative Program on Neutron Scattering is acknowledged.

[1] S. T. Milner and S. A. Safran, Phys. Rev. A **36**, 4371 (1987).
[2] W. Helfrich, Z. Naturforsch. A **28**, 693 (1973).
[3] J. S. Huang, S. T. Milner, B. Farago, and D. Richter, Phys. Rev. Lett. **59**, 2600 (1987).
[4] B. Farago, D. Richter, J. S. Huang, S. A. Safran, and S. T. Milner, Phys. Rev. Lett. **65**, 3348 (1990).
[5] T. Hellweg and D. Langevin, Phys. Rev. E **57**, 6825 (1998).
[6] T. Hellweg and D. Langevin, Physica A **264**, 370 (1999).
[7] T. Hellweg, M. Gradzielski, B. Farago, and D. Langevin, Colloids Surf., A **183–185**, 159 (2001).
[8] V. Lisy and B. Brutovsky, Phys. Rev. E **61**, 4045 (2000).
[9] B. Farago and M. Gradzielski, J. Chem. Phys. **114**, 10105 (2001).
[10] E. Y. Sheu, S. H. Chen, J. S. Huang, and J. C. Sung, Phys. Rev. A **39**, 5867 (1989).
[11] Hu Gang, A. H. Krall, and D. A. Weitz, Phys. Rev. E **52**, 6289 (1995).
[12] M. Nagao, H. Seto, T. Takeda, and Y. Kawabata, J. Chem. Phys. **115**, 10036 (2001).
[13] B. Molle, A. de Geyer, A. Guillermo, and B. Farago, Phys. Rev. Lett. **90**, 068305 (2003).
[14] A. de Geyer, B. Molle, C. Lartigue, A. Guillermo, and B. Farago, Physica B **350**, 200 (2004).
[15] F. Gazeau, F. Boue, E. Dubois, and R. Perzynski, J. Phys.: Condens. Matter **15**, S1305 (2003).
[16] W. Häußler and B. Farago, J. Phys.: Condens. Matter **15**, S197 (2003).
[17] A. L. Rollet, O. Diat, and G. Gebel, J. Phys. Chem. B **106**, 3033 (2002).
[18] M. Nagao, H. Seto, M. Shibayama, and N. L. Yamada, J. Appl. Crystallogr. **36**, 602 (2003).
[19] M. Nagao, H. Seto, and N. L. Yamada, Phys. Rev. E **75**, 061401 (2007).
[20] M. Nagao, H. Seto, M. Shibayama, and T. Takeda, Physica B **385–386**, 783 (2006).
[21] S. W. Lovesey and P. Schofield, J. Phys. C **9**, 2843 (1976).
[22] P. N. Pusey, J. Phys. A **8**, 1433 (1975).
[23] B. J. Ackerson, J. Chem. Phys. **64**, 242 (1976).
[24] B. J. Ackerson, J. Chem. Phys. **69**, 684 (1978).
[25] J. C. Brown, P. N. Pusey, J. W. Goodwin, and R. H. Ottewill, J. Phys. A **8**, 664 (1975).
[26] W. van Megen, I. Snook, and P. N. Pusey, J. Chem. Phys. **78**, 931 (1983).
[27] D. L. Ermak and J. A. McCammon, J. Chem. Phys. **69**, 1352 (1978).
[28] I. Snook, W. van Megen, and R. J. A. Tough, J. Chem. Phys. **78**, 5825 (1983).
[29] J.-Z. Xue, X.-L. Wu, D. J. Pine, and P. M. Chaikin, Phys. Rev. A **45**, 989 (1992).
[30] O. Holderer, H. Frielinghaus, M. Monkenbusch, J. Allgaier, D. Richter, and B. Farago, Eur. Phys. J. E **22**, 157 (2007).
[31] M. Kotlarchyk, S. H. Chen, J. S. Huang, and M. W. Kim, Phys. Rev. Lett. **53**, 941 (1984).
[32] S. H. Chen, S. L. Chang, and R. Strey, J. Chem. Phys. **93**, 1907 (1990).
[33] H. Seto, D. Schwahn, K. Mortensen, and S. Komura, J. Chem. Phys. **99**, 5512 (1993).
[34] H. Seto, D. Schwahn, M. Nagao, E. Yokoi, S. Komura, M. Imai, and K. Mortensen, Phys. Rev. E **54**, 629 (1996).
[35] G. J. M. Koper, W. F. C. Sager, J. Smeets, and D. Bedeaux, J. Phys. Chem. **99**, 13291 (1995).
[36] S. H. Chen, J. Rouch, F. Sciortino, and P. Tartaglia, J. Phys.: Condens. Matter **6**, 10855 (1994).
[37] C. Cametti, P. Codastefano, P. Tartaglia, S. H. Chen, and J. Rouch, Phys. Rev. A **45**, R5358 (1992).
[38] H. Seto, M. Nagao, Y. Kawabata, and T. Takeda, J. Chem. Phys. **115**, 9496 (2001).
[39] T. Takeda, S. Komura, H. Seto, M. Nagai, H. Kobayashi, E. Yokoi, C. M. E. Zeyen, T. Ebisawa, S. Tasaki, Y. Ito, S. Takahashi, and H. Yoshizawa, Nucl. Instrum. Methods Phys. Res. A **364**, 186 (1995).
[40] M. Nagao, N. L. Yamada, Y. Kawabata, H. Seto, H. Yoshizawa, and T. Takeda, Physica B **385–386**, 1118 (2006).
[41] M. Monkenbusch, R. Schätzler, and D. Richter, Nucl. Instrum. Methods Phys. Res. A **399**, 301 (1997).
[42] N. Rosov, S. Rathgeber, and M. Monkenbusch, ACS Symp. Ser. **739**, 103 (2000).
[43] http://www.ncnr.nist.gov/dave
[44] P. G. de Gennes, Physica (Amsterdam) **25**, 825 (1959).
[45] Y. Kawabata, H. Seto, M. Nagao, and T. Takeda, J. Chem. Phys. **127**, 044705 (2007).
[46] K. Seki and S. Komura, Physica A **219**, 253 (1995).
[47] S. F. Edwards and M. Schwartz, Physica A **167**, 595 (1990).
[48] N. F. Carnahan and K. E. Starling, J. Chem. Phys. **51**, 635 (1969).
[49] J. F. Brady, J. Chem. Phys. **99**, 567 (1993).
[50] Y. Kawabata, M. Nagao, H. Seto, S. Komura, T. Takeda, D. Schwahn, N. L. Yamada, and H. Nobutou, Phys. Rev. Lett. **92**, 056103 (2004).
[51] Y. Kawabata, H. Seto, M. Nagao, and T. Takeda, J. Neutron Res. **10**, 131 (2002).
[52] B. P. Binks, H. Kellay and J. Meunier, Europhys. Lett. **16**, 53 (1991).